Design of Robust SMES Controller in a Multimachine Power System by using Hybrid TS/EP

S. Dechanupaprittha, K. Hongesombut, M. Watanabe, Y. Mitani and I. Ngamroo*
Kyushu Institute of Technology, Kitakyushu, Japan 804-8550
d300404d@tobata.isc.kyutech.ac.jp
*Sirindhorn International Institute of Technology, Thammasat University, Pathumthani, Thailand 12121

Abstract - This paper proposes the design of robust superconducting magnetic energy storage (SMES) controller in a multimachine power system by using hybrid tabu search and evolutionary programming (Hybrid TS/EP). The multimachine power system and the SMES with controller are formulated as an optimization problem. The proposed objective function not only considers the disturbance attenuation performance but also the robust stability index. Subsequently, the robust SMES controller for active and reactive power control are designed systematically by using Hybrid TS/EP in order to improve the power system damping and the robustness against system uncertainties. Consequently, nonlinear simulation studies under various situations are carried out to exhibit and confirm the effectiveness and robustness of the designed robust SMES controller.

Keywords - Robust controller design, superconducting magnetic energy storage, multiplicative stability margin, tabu search, evolutionary programming

1 INTRODUCTION

NOWADAYS , a practical power system associated with several machines is confronted with the presence of electromechanical oscillation (EMO) modes. These EMO modes (0.2-2.5 Hz) are often poorly damped due to the limit on a maximum power transfer in transmission lines and the complexity of a power system network. In particular, the insufficient damping of such complex EMO modes usually causes unavoidable low frequency oscillations following unexpected disturbances [1]-[3].

The superconducting magnetic energy storage (SMES) unit is regarded as an effective energy storage device for leveling load demands and compensating for load changes. In particular, it is capable of supplying or receiving the active and reactive power simultaneously as well as stabilizing the power system. The applications of superconducting magnetic energy storage (SMES) to enhance the power system damping were studied by many researchers [4]-[7]. Recently, the controller design of SMES active and reactive power for improving the transient stability of power system presented by [8]-[10] show that a proper modulation control of SMES active and reactive power can overcome the problem of low frequency oscillations.

This paper proposes the design of robust superconducting magnetic energy storage (SMES) controller in a multimachine power system using a heuristic optimization method. The fast control of SMES unit is one sophisticated advantage that can be utilized to alleviate the problem of system transient instability due to undesirable disturbances. The proposed design considers the SMES unit with simultaneous active and reactive power control. In particular, a model of SMES coil current, which is the permissible range of SMES operation, is also taken into account to realize its characteristics during operations. Moreover, a multiplicative uncertainty model included in the proposed design method can be used to determine the multiplicative stability margin (MSM), which can be regarded as the robust stability margin.

To obtain the parameters of SMES controller, the multimachine power system and the SMES with controller are formulated as an optimization problem. The proposed objective function not only considers the disturbance attenuation performance but also the robust stability margin. Subsequently, the robust controllers of SMES active and reactive power are designed systematically by using hybrid tabu search and evolutionary programming (Hybrid TS/EP) in order to improve the power system damping and the robustness against system uncertainties. Consequently, non-linear time-domain simulation studies are carried out to exhibit and confirm the effectiveness and robustness of the designed robust SMES controller in a multimachine power system under various situations.

The organization of this paper is as follows. Sections 2 and 3 describe the study system and the control problem formulation, respectively. Next, Hybrid TS/EP is explained in Section 4. Subsequently, the results and evaluations are carried out in Section 5. Finally, conclusions are given in Section 6.

2 STUDY SYSTEM

2.1 Linearized Power System Model

The study power system consists of two machines connected to an infinite bus as illustrated in Fig. 1. It is represented by a linearized model around a design operation condition (DOC). Each generator model is represented by

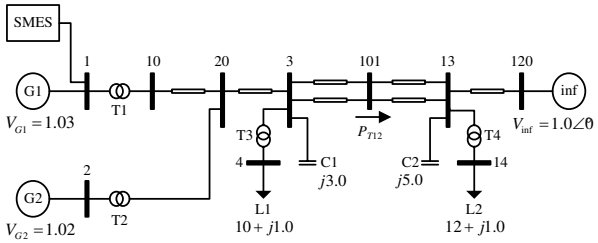

Figure 1: Two-machine infinite bus power system.

a 4-state transient model and is equipped with a simplified exciter [3]. The state equations of a linearized power system (A_S, B_S, C_S, D_S) in Fig. 1 can be expressed as

$$\begin{aligned} \Delta\dot{x} &= A_S\Delta x + B_S\Delta u_{CTL}, \\ \Delta y &= C_S\Delta x + D_S\Delta u_{CTL}, \\ \Delta u_{CTL} &= K_{CTL}\Delta u_{IN}, \end{aligned} \tag{1}$$

where, $\Delta x = \left[\ \Delta\delta \quad \Delta\omega \quad \Delta e'_d \quad \Delta e'_q \quad \Delta E_{fd}\ \right]^T$, $(5n\times 1)$; Δy is the output signal of system, $(2m\times 1)$; $\Delta\delta$ denotes the deviation of rotor angle, $(n\times 1)$; $\Delta\omega$ is the deviation of rotor speed, $(n\times 1)$; $\Delta e'_d$ and $\Delta e'_q$ are the deviations of transient internal voltages of a generator in d-axis and q-axis, respectively, $(n\times 1)$; ΔE_{fd} is the deviation of field voltage, $(n\times 1)$; K_{CTL} is the SMES with active and reactive power (P-Q) controllers, $(2m\times 2m)$; Δu_{CTL} is the control output signal of K_{CTL}, $(2m\times 1)$; Δu_{IN} is the feedback input signal of K_{CTL}, $(2m\times 1)$; n and m are the numbers of machines and SMESs, respectively. Note that the system (1) is a multi-input multi-output (MIMO) control system and is referred to as the nominal plant G.

2.2 SMES Model and Control Scheme

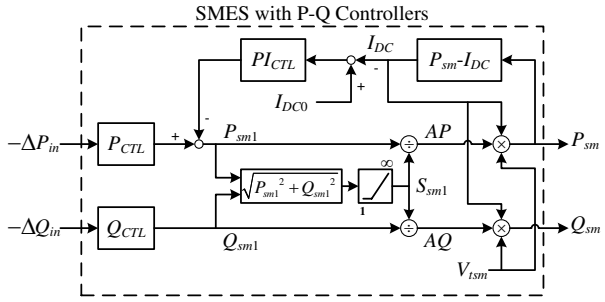

Figure 2: SMES with P-Q controllers.

The SMES model with active and reactive power modulation control scheme, as depicted in Fig. 2, is used in this paper. In particular, each SMES unit includes two controllers of P_{CTL} and Q_{CTL}, where, P_{CTL} and Q_{CTL} are the SMES active power controller and SMES reactive power controller, respectively. The SMES with P-Q controllers is obviously an MIMO system. Moreover, the effect of SMES coil current is included to realize its characteristics during operations. In practice, the SMES coil current (I_{DC}) is not allowed to reach zero to prevent the possibility of discontinuous conduction under unexpected disturbances. Based on the hardware operational constraints, the lower and upper coil current limits are $0.30I_{DC0}$ and $1.38I_{DC0}$, respectively [5], where, I_{DC0} is an initial value of SMES coil current. In addition, the PI_{CTL} is a proportional-integral controller used to stabilize the SMES coil current.

The SMES output active power (P_{sm}) and SMES output reactive power (Q_{sm}) can be expressed as

$$P_{sm} = V_{tsm}I_{DC}AP, \tag{2}$$

$$Q_{sm} = V_{tsm}I_{DC}AQ, \tag{3}$$

where, AP and AQ are the active and reactive power fractions, respectively. For simplicity, V_{tsm} is assumed as a terminal voltage of SMES unit, (pu). For $P_{sm} - I_{DC}$ in Fig. 2, it represents the relationship between the current I_{DC} and the sensed P_{sm}. In particular, I_{DC} can be calculated by (4) and (5) as follows,

$$E_{out} = \int P_{sm}dt \cdot S_{sm,base}, \tag{4}$$

$$I_{DC} = \sqrt{I_{DC0}^2 - \frac{2E_{out}}{L_{sm}\cdot I_{sm,base}^2}}, \tag{5}$$

where, L_{sm} is the SMES coil inductance, (H); E_{out} is the SMES energy output, (J); $I_{sm,base}$ is the SMES current base, (A); and $S_{sm,base}$ is the SMES MVAbase, (MVA). Subsequently, the energy stored in the SMES unit (E_{sm}) and the initial E_{sm} (E_{sm0}) can be determined by (6) and (7) as follows,

$$E_{sm} = E_{sm0} - E_{out}, \tag{6}$$

$$E_{sm0} = \frac{1}{2}L_{sm}I_{DC0}^2 \cdot I_{sm,base}^2. \tag{7}$$

Normally, the SMES unit should not supply/receive active and reactive power to/from the power system. On the other hand, the SMES unit should alleviate power system oscillations following disturbances.

3 CONTROL PROBLEM FORMULATION

3.1 Controller Structure

The structure of controller for P_{CTL} and Q_{CTL} is in a form of a lead/lag controller as

$$\Delta u_{CTL} = K_C \cdot \frac{sT_w}{1+sT_w} \cdot \frac{1+sT_1}{1+sT_2} \cdot \Delta u_{IN}, \tag{8}$$

where, K_C is a controller gain; T_w is a wash-out time constant; and, T_1 and T_2 are controller time constants. Note that Δu_{IN} for P_{CTL} is an active power deviation (ΔP_{in}), and Δu_{IN} for Q_{CTL} is a reactive power deviation (ΔQ_{in}).

In this paper, T_w is set to 5 s. The control parameters, i.e. K_C, T_1 and T_2, for P_{CTL} and Q_{CTL} are searched simultaneously based on the objective function explained in the following subsection.

3.2 Determination of Objective Function

In derivation of the objective function, both attenuation performance of system disturbance and robust stability of control system against system uncertainties are taken into consideration. Since the main purpose of the proposed design method is to improve the system damping following any disturbances, therefore, the damping ratio (ζ) of EMO mode is used as a design specification. Assuming that eigenvalues corresponding to the mode of oscillation can be determined as $-\sigma \pm j\omega_d$, the damping ratio is given by

$$\zeta_{actual} = \frac{-\sigma}{\sqrt{\sigma^2+\omega_d^2}}. \tag{9}$$

The desired damping ratio of the eigenvalues corresponding to the mode of oscillation is specified as $\zeta_{desired}$. Accordingly, the difference between the desired and the actual damping ratios can be defined as

$$\psi = |\zeta_{desired} - \zeta_{actual}| \,. \tag{10}$$

Note that the disturbance attenuation performance increases when ψ is minimized.

Here, the D-Stability region is used to guarantee the desired damping ratio and the real part of EMO mode. As shown in Fig. 3, ζ_0 and σ_0 are set at 10 % and -0.5, respectively.

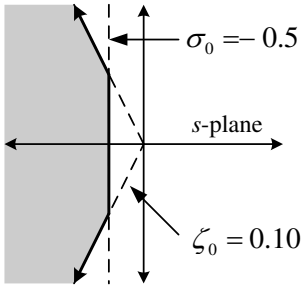

Figure 3: D-Stability region.

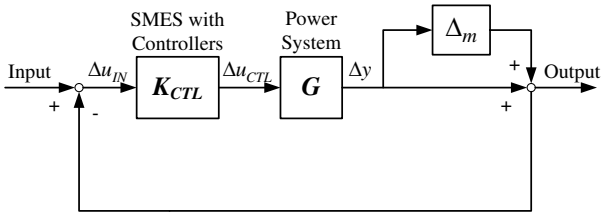

Figure 4: Feedback system with multiplicative uncertainty.

For the robust stability of a system, the plant uncertainty is modeled as a multiplicative form [11] demonstrated in Fig. 4. Δ_m is a stable multiplicative uncertainty. Based on the small-gain theorem, the closed loop system will be robustly stable if

$$|\Delta_m| < \frac{1}{|G \cdot K_{CTL}(1 + G \cdot K_{CTL})^{-1}|}, \tag{11}$$

where, the symbol $|\bullet|$ shows the magnitude of transfer function $(\bullet)$. Note that $T = G \cdot K_{CTL}(1+G \cdot K_{CTL})^{-1}$ is the complementary sensitivity function, or the closed-loop transfer function. Based on this uncertainty representation, the robust stability margin can be determined in term of MSM. In other words, MSM also implies the maximum uncertainty bound and can be calculated by

$$\text{MSM} = 1/\left\|T\right\|_\infty , \tag{12}$$

where, $\left\|T\right\|_\infty$ is the ∞-norm of T. From (11) and (12), it is clear that by minimizing $\left\|T\right\|_\infty$, the robust stability margin will be improved as the MSM increases [11]. Thus, the normalized robustness index of the objective function is defined as

$$\gamma = \left\|T\right\|_\infty / \left\|T\right\|_{\infty(initial)} , \tag{13}$$

where, $\left\|T\right\|_{\infty(initial)}$ is the specified ∞-norm of T at an initial of a search process.

Combining (10) and (13), the control problem can be formulated as the following optimization problem,

$$\begin{aligned} \min \quad & C\left(K_C, T_j\right) = \psi + \gamma, \\ \text{st.} \quad & K_{\min} \le K_C \le K_{\max}, \\ & T_{\min} \le T_j \le T_{\max}, \quad j = 1, 2 \end{aligned} \tag{14}$$

where, $C(K_C, T_j)$ is the objective function. The minimum and maximum values of the gain K_C are set as 1 and 100, respectively. The minimum and maximum values of the time constants T_j are set as 0.001 and 10, respectively. In this paper, the hybrid tabu search and evolutionary programming method (Hybrid TS/EP) introduced by [12] is applied to solve the optimization problem.

4 HYBRID TABU SEARCH AND EVOLUTIONARY PROGRAMMING

4.1 Initialization

The actual values of the N parameters, P_i, i = 1, ..., N, are randomly generated between the minimum actual parameters ($P_{i,\min}$) and the maximum actual parameters ($P_{i,\max}$) of the k-th individual solution, $X_k = [P_1^k, \ldots, P_i^k, \ldots, P_N^k]$, $k = 1, \ldots, NP$, where, NP is the population size. After initializing the individual solutions in the population, the objective function in (14) is used to verify the quality of initial individuals. The best initial individual is recorded into the tabu list (to be discussed in Subsection 4.3).

Furthermore, for each generation, Hybrid TS/EP performs 5 operations: perturbation strategies, tabu list restriction, fitness function evaluation, rank selection with elitism, and adaptive parameter setting strategies (to be discussed in Subsection 4.2, 4.3, 4.4, and 4.5, respectively).

4.2 Perturbation Strategies

In this paper, Hybrid TS/EP uses mutation as a diversification searching strategy and arithmetic crossover [13] operator as an intensification searching strategy to obtain the optimal or near optimal solution [12].

4.2.1 Mutation

The offspring individuals (the new trial solutions) obtained from mutation process, $X_k^{new} = [P_1^{k,new}, \ldots, P_i^{k,new}, \ldots, P_N^{k,new}], k = 1, \ldots, N_m$, are defined as

$$P_i^{k,new} = P_i^k + H(0, \mu_i), \quad i = 1, \ldots, N, \tag{15}$$

where, P_i^k is the actual value of the i-th parameter of the k-th parent individual; $H(0, \mu_i)$ is a uniform random variable with variance μ_i; μ_i is $|C_k/C_{\max}|(P_{i,\max} - P_{i,\min})\beta$, $i = 1, \ldots, N$; β is an adaptive mutation scale; N_m is the number of mutated individuals; C_k is the objective value of the k-th parent individual; $C_{\max}$ is the maximum objective value in the parent population. Note that if $P_i^{k,new}$ is higher or lower than its operating limits, set it to the limit.

4.2.2 Arithmetic Crossover

Based on the inherited genotypes of two randomly selected parent individuals X_{k1} and X_{k2}, the offspring individuals obtained from the arithmetic crossover, $X_k^{new} = [P_1^{k,new}, \ldots, P_i^{k,new}, \ldots, P_N^{k,new}]$, $k = N_m + 1, \ldots, NP$, are formulated by

$$X_k^{new} = X_{k1} + u \cdot (X_{k2} - X_{k1}), \tag{16}$$

where, u is defined as a uniform random number ranges from zero to one.

4.3 Tabu List Restriction

The tabu list (TL) is used to keep best offspring individuals (solution vectors) in past iterations. During the search process, a new solution vector enters TL and the oldest one is released, as shown in Fig. 5. In particular, this technique prevents a cycling of visited offspring individuals in the perturbation process by forbidding perturbed individuals, which are similar to those in TL, from being used as solution candidates [14].

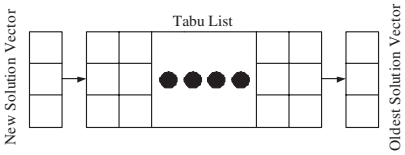

Figure 5: Mechanism of Tabu List.

In general, if the size of TL is too small, the cycling of solution occurs in the search process. On the other hand, if the size is too large, the search process is in less diversity. Hence, the appropriate size in our application is between 7 and 30.

For each generation counter g, the tabu list size (TLS) must be satisfied under the condition, $0 \leq TLS \leq \tau(g)$. $\tau(g)$ is the maximum allowable TLS (to be discussed in subsection 4.5). The tabu restriction for the k-th individual, $k = 1, \ldots, NP$ can be expressed as

$$\begin{aligned} \sqrt{\sum_{i=1}^{N} \left(\frac{P_i^{k,new} - P_i^{tabu,t}}{P_{i,\max} - P_{i,\min}} \right)^2} &< (d_0 \cdot \eta^g \triangleq d_{tabu}), \\ t &= 1, \ldots, TLS, \end{aligned} \tag{17}$$

where, d_{tabu} is the tabu distance; d_0 is the initial value of tabu distance $(= 5 \times 10^{-4})$; η is the drop factor (= 0.95); $P_i^{tabu,t}$ is the actual value of the i-th parameter of the t-th tabued solution in TL.

At the beginning, a higher d_{tabu} is used to provide diversification in order to reduce the search effort towards the optimal region. Moreover, the intensification will occur when the generation counter g reaches the maximum generation limit, $g_{\max}$.

4.4 Fitness Function Evaluation and Rank Selection with Elitism

The fitness function is evaluated based on a distance term and an objective function term. Accordingly, the fitness function can be formulated by

$$\begin{aligned} F_k &= 4 \cdot NP - (RC_k + \alpha \cdot RD_k), \\ &\quad k = 1, \ldots, 2 \times NP, \end{aligned} \tag{18}$$

where, F_k is the fitness score of the k-th individual,$k = 1, \ldots, 2 \times NP$; α is an adaptive decay scale, which can be obtained from (21); RC_k is the integer rank score of C_k of the k-th individual can be assigned by the lowest score (= 1) for the lowest C_k and the highest score $(= 2 \times NP)$ for the highest C_k; RD_k is the integer rank score of D_k of the k-th individual can be assigned by the lowest score (= 1) for the highest D_k and the highest score $(= 2 \times NP)$ for the lowest D_k; C_k is the objective value of the k-th individual.

D_k, the summation of distance between the k-th individual and each visited solution vector in TL, can be expressed as

$$D_k = \sum_{t=1}^{TLS} \sqrt{\sum_{i=1}^{N} \left(\frac{P_i^k - P_i^{tabu,t}}{P_{i,\max} - P_{i,\min}} \right)^2}, \tag{19}$$

where, P_i^k is the actual value of the i-th parameter of the k-th individual. With the rank selection operator, the NP highest fitness score individuals will be chosen as parent individuals for next generation. Those individuals are obtained from a combined population $(2 \times NP)$ of the old parent population and the offspring population. This strategy is used to avoid the premature convergence of solution.

Moreover, if a new parent population for the next generation does not contain the current best individual, the elitism will replace the last individual in a new parent population by the current best individual. This technique guarantees the current best individual surviving until the last generation.

4.5 Adaptive Parameter Setting Strategies

4.5.1 Determination of N_m and N_c

The parameters setting for N_m and N_c must satisfy the condition

$$N_m + N_c = NP, \tag{20}$$

where, $0 \leq N_m \leq NP$ and $0 \leq N_c \leq NP$.

Initially, both parameters are set to 50 % of NP. For the next generation, if the best offspring individual is better than the best parent individual by mutation (or crossover) process, the parameter N_m (or N_c) for the next generation will be increased by the intensification number (I). I is set to 20 % of NP. N_c is the number of arithmetic crossover individuals.

Otherwise, if the best offspring individual does not improve solution quality better than the best parent individual, then both parameter settings of N_m and N_c for the next generation will be recovered to the old generation parameter settings.

$$S(g+1) = \begin{cases} \text{Max}\{S_{\min}, S(g) - S_{\Delta}\} & ; \text{if } C_{\min}(g) = C_{\min}(g-1) \\ S(g) & ; \text{if } C_{\min}(g) < C_{\min}(g-1) \end{cases} \quad (21)$$

4.5.2 Determination of α, β and τ

The parameters setting of α, β, and τ, represented by S, can be formulated by (21). S_{Δ} is the step size related to each parameter. $C_{\min}(g)$ is the objective value of the best offspring individual at the generation counter g. At the beginning, S is set to the maximum value of parameter setting. For the next generation, S is controlled by the generation counter g.

In this paper, $\beta_{\min}$, $\beta_{\max}$, and β_{Δ} are set to 0.005, 0.5, and 0.025, respectively. $\alpha_{\min}$, $\alpha_{\max}$, and α_{Δ} are set to 0.005, 0.5, and 0.025, respectively. $\tau_{\min}$, $\tau_{\max}$, and τ_{Δ} are set to 7, 30, and 1, respectively.

4.6 Hybrid TS/EP Procedure

The Hybrid TS/EP procedure can be described as follows:

Step 1: Read the system data, and specify the parameter settings of Hybrid TS/EP.

Step 2: Initialize the initial individuals, $X_k, k = 1, \ldots, NP$ and the design specification. Evaluate the objective function (C_k) in (14), and update tabu list (TL).

Step 3: Initialize the generation counter g to zero.

Step 4: Execute Hybrid TS/EP operators as follow:

- *Step 4.1*: Perform the perturbation strategies.
  - *Step 4.1.1*: Initialize the individual counter k to one.
  - *Step 4.1.2*: Perform the mutation based on TL restriction until the k-th offspring individual does not satisfy TL restriction in (17).
  - *Step 4.1.3*: If $k < N_m$, increase the individual counter k by one and go to Step 4.1.2.
  - *Step 4.1.4*: Initialize individual counter k to N_m+1.
  - *Step 4.1.5*: Perform the arithmetic crossover based on TL restriction until the k-th offspring individual does not satisfy TL restriction in (17).
  - *Step 4.1.6*: If $k < NP$, increase the individual counter k by one and go to Step 4.1.5.
- *Step 4.2*: Combine the offspring population and parent population into a single population to evaluate the objective value and fitness of each individual.
- *Step 4.3*: Perform the rank selection with elitism mechanism to update the new parent individuals from a combined population of the old parent population and offspring population for the next generation.
- *Step 4.4*: Perform the adaptive parameter setting strategies and update TL.
- *Step 4.5*: If the generation counter g is less than the maximum generation limit $g_{\max}$, increase generation counter g by one and go to Step 4.

Step 5: Hybrid TS/EP is terminated and the current best individual is a solution for the robust design.

5 RESULTS AND EVALUATIONS

To demonstrate the effectiveness of the designed robust SMES controller (RSMES), including P_{CTL} and Q_{CTL}, the study system of two-machine connected to an infinite bus, as shown in Fig. 1, is used. All system data are given in the Appendix. By observing participation factors of the dominant EMO mode, the SMES unit with P-Q controller is installed at machine 1 [3]. In addition, the deviations of active and reactive power generated by machine 1 are used as input signals of the SMES controller. The proposed robust design method based Hybrid TS/EP is developed via MATLAB programming language. The computer used is a Pentium4-3.0 GHz PC with RAM 1.0 GBytes. The control parameters of the RSMES are searched using the proposed objective function (14) following the design procedure. NP and g_{max} are set to 100 and 480, respectively. The desired damping ratio $\zeta_{desired}$ = 0.2 is appointed. As results, the total computational time for the search process is 4,522 s. The RSMES of P_{CTL} and Q_{CTL} is obtained as below,

$$P_{CTL} : 13.752 \cdot \frac{5s}{1+5s} \cdot \frac{1+0.0485s}{1+0.7948s}, \quad (22a)$$

$$Q_{CTL} : 1.0 \cdot \frac{5s}{1+5s} \cdot \frac{1+0.2265s}{1+2.1619s}. \quad (22b)$$

The RSMES is examined under four different operating conditions as given in Table 1. For comparison purpose, the conventional SMES controller (CSMES) is given. The P_{CTL} of CSMES is $16(0.01s+1)/(1.0s+1)$ and the Q_{CTL} of CSMES is $1.0(0.01s+1)/(1.0s+1)$. Note that the CSMES is designed manually at the design operating condition (DOC) to yield the damping ratio of the dominant EMO mode of 0.2, which is the same as the design specification of the RSMES. However, the MSM is not considered in the design of CSMES.

Case study	P_{G1} (pu)	P_{G2} (pu)	P_{L1} (pu)	P_{T12} (pu)	Line outage
DOC	5.5	5.5	10	0.8	-
1	5.0	5.0	5	4.8	-
2	5.5	5.5	6	4.8	-
3	6.5	6.5	10	2.8	101-13 (1 circuit)

Table 1: Operating Conditions.

Case study	No SMES	CSMES	**RSMES**
DOC	-0.028$\pm j$3.079, 0.0091	-0.639$\pm j$3.185, 0.1968	**-0.618$\pm j$3.027, 0.1999**
1	0.060$\pm j$2.871, -0.0209	-0.447$\pm j$2.970, 0.1488	**-0.444$\pm j$2.853, 0.1539**
2	0.089$\pm j$2.830, -0.0314	-0.401$\pm j$2.932, 0.1355	**-0.402$\pm j$2.823, 0.1411**
3	0.093$\pm j$2.345, -0.0395	-0.244$\pm j$2.356, 0.1029	**-0.236$\pm j$2.300, 0.1020**

Table 2: Dominant modes and damping ratios.

The eigenvalues and damping ratios of the dominant EMO modes for all case studies are given in Table 2. For all case studies, the damping ratios of EMO modes for the case of RSMES and CSMES are slightly different and all of them are in the D-Stability region. This implies that for small disturbances the damping performance by RSMES and CSMES should be similar.

Case study	CSMES	**RSMES**
DOC	0.0827	**0.1947**
1	0.0832	**0.1951**
2	0.0827	**0.1945**
3	0.0815	**0.1932**

Table 3: Multiplicative stability margins (MSMs).

Table 3 shows the values of MSM, which is the robust stability margin, for each case study. Obviously, the MSMs of the power system with RSMES are at the higher value. The MSM indicates the ability of control system to guarantee some degree of system uncertainties. The higher the MSM, the better robust stability will be.

Next, non-linear simulation studies are carried out to show the robustness of the power system with RSMES in comparison with CSMES by using Dymola [15]. Under four operating conditions given in Table 1, it is assumed that there is a disturbance occurred for each case study. For Case study DOC and 1, there is a three-phase fault to ground at bus 20 for 20 ms and 50 ms, respectively. There is no line removed after the fault is cleared. As shown in Fig. 6 and 7, both RSMES and CSMES can successfully damp out the oscillation. However, the SMES without P-Q controllers (NoSMES), the power system becomes unstable as in Fig. 7.

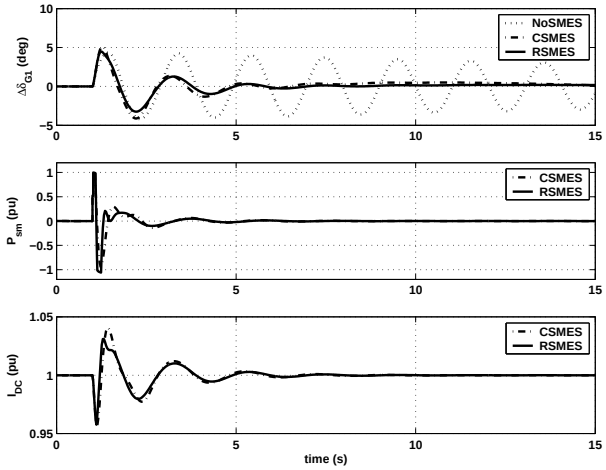

Figure 6: System responses of Case study DOC.

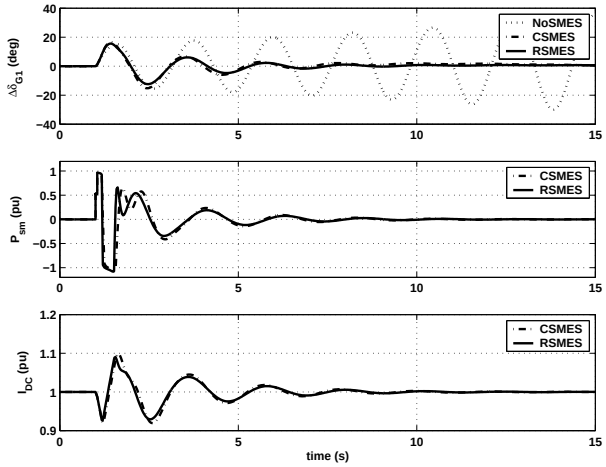

Figure 7: System responses of Case study 1.

For Case study 2, the transmission system is at the heavy load condition as in Case study 1. However, the point is that how the sudden configuration changes affect the stability of a power system. In addition, the system with CSMES provides a degree of stability margin (MSM) lower than the system with RSMES. It is assumed that one circuit of line 101-13 is tripped temporarily without fault for 1.2 s and is then reclosed back into service. Consequently, the CSMES cannot provide enough damping performance to the power system and lose the synchronism. On the other hand, the RSMES can effectively maintain the stability of the power system as shown in Fig. 8.

For Case study 3, there is one circuit of line 101-13 out-of-service. Accordingly, the tie-line becomes weaker. Subsequently, the three-phase fault to ground is occurred in the middle of line 101-13 for 70 ms. The line is reclosed after the fault is cleared for 200 ms. Apparently, as exhibited in Fig. 9, the CSMES loses its control but the RSMES still robustly retain the power system stability successfully.

The RSMES improves the system damping performance and also yields larger MSMs compared with the system with CSMES. With the larger MSM, the system

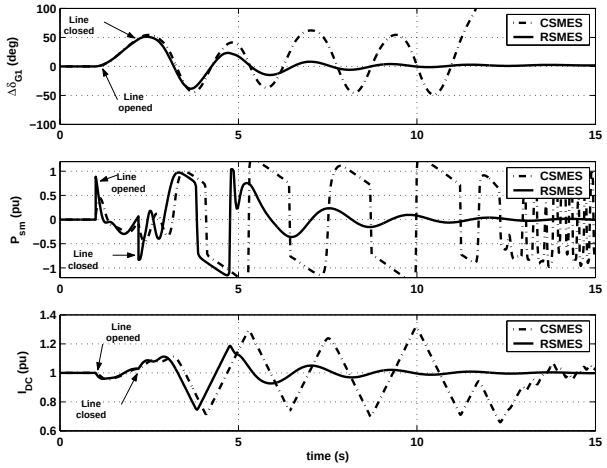

Figure 8: System responses of Case study 2.

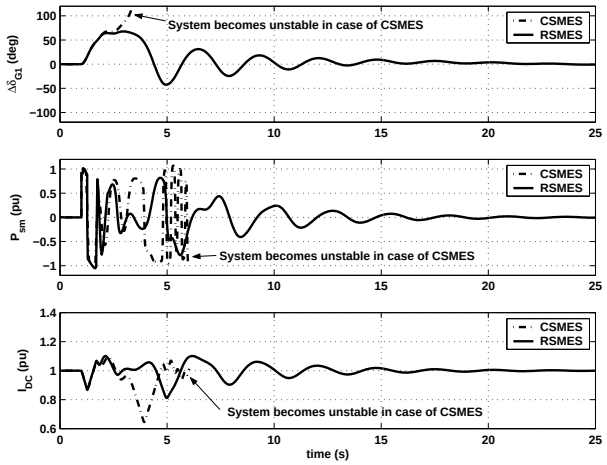

Figure 9: System responses of Case study 3.

can deal with a higher degree of system variations at which the system can insist without destabilized by unexpected disturbances. With a proper design specification, the proposed design method can also be applied to a larger system. In particular, comprehensive engineering backgrounds is not required by the proposed design method. The control parameters are automatically searched and obtained with appropriate design constraints. It should also be noted that the computational time for the search process does not affect the quality of solution. In addition, I_{DC} is effectively regulated during power system oscillations following disturbances and is significantly remained within the constraints for all cases.

6 CONCLUSIONS

In this paper, the design of robust SMES controller in a multimachine power system is proposed. The SMES active and reactive power controllers are designed simultaneously to yield the desired damping performance. Meanwhile, the robust stability margin is improved. Automatically, the control parameters are searched and obtained with less effort by using Hybrid TS/EP. With proper design specifications, the SMES with P-Q controllers can effectively damp out power system oscillations following severe disturbances. Moreover, the improvement of robust stability margin, or MSM, allows the power system to insist a more serious situation. Finally, simulation studies reveal that the designed robust SMES controller provides the power system with the robust damping performance and robust stability against system uncertainties.

Appendix: System Data

SystemBase: 100 MVA

Generator (MVAbase=900) and Exciter

H	x_d	x_q	x'_d	x'_q	T'_{d0}	T'_{q0}	K_a	T_a
6.5	1.8	1.7	0.3	0.55	8	0.4	200	0.05

Note: E_{fd} limits are $\pm$5.0 pu.

Transmission line

From	To	R	X	B	Tab
1	10	0	0.0167	0	1.0
10	20	0.0025	0.025	0.0437	-
2	20	0	0.0167	0	1.0
20	3	0.001	0.01	0.0175	-
3	101	0.011	0.11	0.1925	-
3	101	0.011	0.11	0.1925	-
3	4	0	0.005	0	1.0
101	13	0.011	0.11	0.1925	-
101	13	0.011	0.11	0.1925	-
13	14	0	0.005	0	1.0
13	120	0.001	0.01	0.0175	-

SMES

$S_{sm,base}$	$I_{sm,base}$	I_{DC0}	L_{sm}	K_P	T_I
100	4,545	1.0	10	40	0.4

Note: K_P and T_I are parameters of PI_{CTL} in Fig. 2.

REFERENCES

[1] P. Kundur, “Power System Stability and Control”, New York, McGraw Hill, 1994

[2] J. Machowski, J. Bialek and J. Bumby, “Power System Dynamics and Stability”, New York, Wiley, 1997

[3] G. Rogers, “Power System Oscillations”, Kluwer Academic Publishers, 2000

[4] Y. Mitani, K. Tsuji and Y. Murakami, “Application of Superconducting Magnetic Energy Storage to Improve Power System Dynamic Performance”, IEEE Trans. on Power Systems, vol. 3, no. 4, pp. 1418-1425, 1989

[5] C. J. Wu and Y. S. Lee, “Application of Superconducting Magnetic Energy Storage Unit to Improve the Damping of Synchronous Generator”, IEEE Trans. on Energy Conversion, vol. 6, no. 4, pp. 573-578, 1991

[6] M. G. Rabbani, J. B. X. Devotta and S. Elangovan, “Application of Simultaneous Active and Reactive Power Modulation of SMES Unit under Unequal α-mode for Power System Stabilization”, IEEE Trans. on Power Systems, vol. 14, no. 2, pp. 547-552, 1999

[7] J. B. X. Devotta and M. G. Rabbani, “Application of Superconducting Magnetic Energy Storage Unit in Multimachine Power Systems”, Energy Conversion and Management, vol. 41, no. 5, pp. 493-504, 2000

[8] Y. Lee, “Superconducting Magnetic Energy Storage Controller Design and Stability Analysis for a Power System with Various Load Characteristics”, Electric Power Systems Research, vol. 51, no. 1, pp. 33-41, 1999

[9] B. C. Pal, A. H. Coonick, I. M. Jaimoukha and H. El-Zobaidi, “A Linear Matrix Inequality Approach to Robust Damping Control Damping in Power Systems with Superconducting Magnetic Energy Storage Device”, IEEE Trans. on Power Systems, vol. 15, no. 1, pp. 356-362, 2000

[10] B. C. Pal, A. H. Coonick and D. C. Macdonald, “Robust Damping Controller Design in Power System with Superconducting Magnetic Energy Storage Devices”, IEEE Trans. on Power Systems, vol. 15, no. 1, pp. 320-325, 2000

[11] B. Shahian and M. Hassul, “Control System Design using MATLAB”, New Jersey, Prentice Hall, 1993

[12] W.-M. Lin, F.-S. Cheng and M.-T. Tsay, “An Improved Tabu Search for Economic Dispatch with Multiple minima”, IEEE Trans. on Power Systems, vol. 17, no. 1, pp. 108-112, 2002

[13] M. Gen and R. Cheng, “Genetic Algorithms and Engineering Design”, New York, John Wiley & Sons, 1997

[14] F. Glover and M. Laguna, “Tabu Search”, London, Kluwer Academic Publishers, 2001

[15] K. Hongesombut, Y. Mitani and K. Tsuji, “An Incorporated Use of Genetic Algorithm and a Modelica Library for Simultaneous Tuning of Power System Stabilizers”, 2^{nd} Int. Modelica Conf. Proceedings, pp. 89-98, 2002